Exploring Energy Landscapes

Objective: to exploit stationary points (minima and transition states) of the PES as a computational framework (*J. Phys. Chem. B*, **110**, 20765, 2006):

- Basin-hopping for global optimisation (*J. Phys. Chem. A*, **101**, 5111 1997).
  The landscape is transformed via local minimisation: $\widetilde{E}(\mathbf{X}) = \min E(\mathbf{X})$.
  Steps are proposed via geometrical perturbations, and accepted or rejected according to criteria such as the change in energy, e.g. via Metropolis.
- Basin-sampling for global thermodynamics (*J. Chem. Phys.*, **124**, 044102, 2006).
  This approach uses the superposition method, where the total partition function is written as a sum over minima, $Z(T) = \sum_a Z_a(T)$.
- Discrete path sampling for global kinetics (*Mol. Phys.*, **100**, 3285, 2002).
  Transition state searches are used to construct a kinetic transition network. Rate constants are extracted assuming Markovian dynamics and a unimolecular rate theory for individual minimum-to-minimum transitions.

Exploring Energy Landscapes

Objective: to exploit stationary points (minima and transition states) of the PES as a computational framework (*J. Phys. Chem. B*, **110**, 20765, 2006):

- Basin-hopping for global optimisation (*J. Phys. Chem. A*, **101**, 5111 1997).
  The landscape is transformed via local minimisation: $\widetilde{E}(\mathbf{X}) = \min E(\mathbf{X})$.
  Steps are proposed via geometrical perturbations, and accepted or rejected according to criteria such as the change in energy, e.g. via Metropolis.
- Basin-sampling for global thermodynamics (*J. Chem. Phys.*, **124**, 044102, 2006).
  This approach uses the superposition method, where the total partition function is written as a sum over minima, $Z(T) = \sum_a Z_a(T)$.
- Discrete path sampling for global kinetics (*Mol. Phys.*, **100**, 3285, 2002).
  Transition state searches are used to construct a kinetic transition network. Rate constants are extracted assuming Markovian dynamics and a unimolecular rate theory for individual minimum-to-minimum transitions.

Thermodynamics for Ala_4 in Vacuum: CHARMM

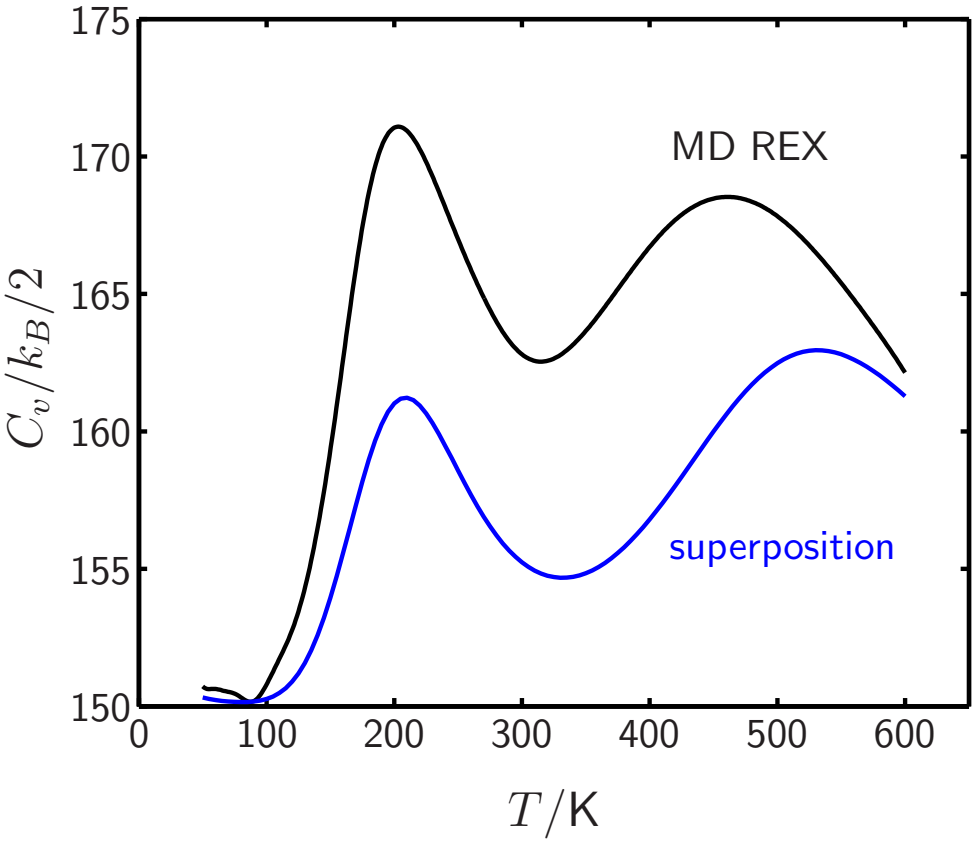

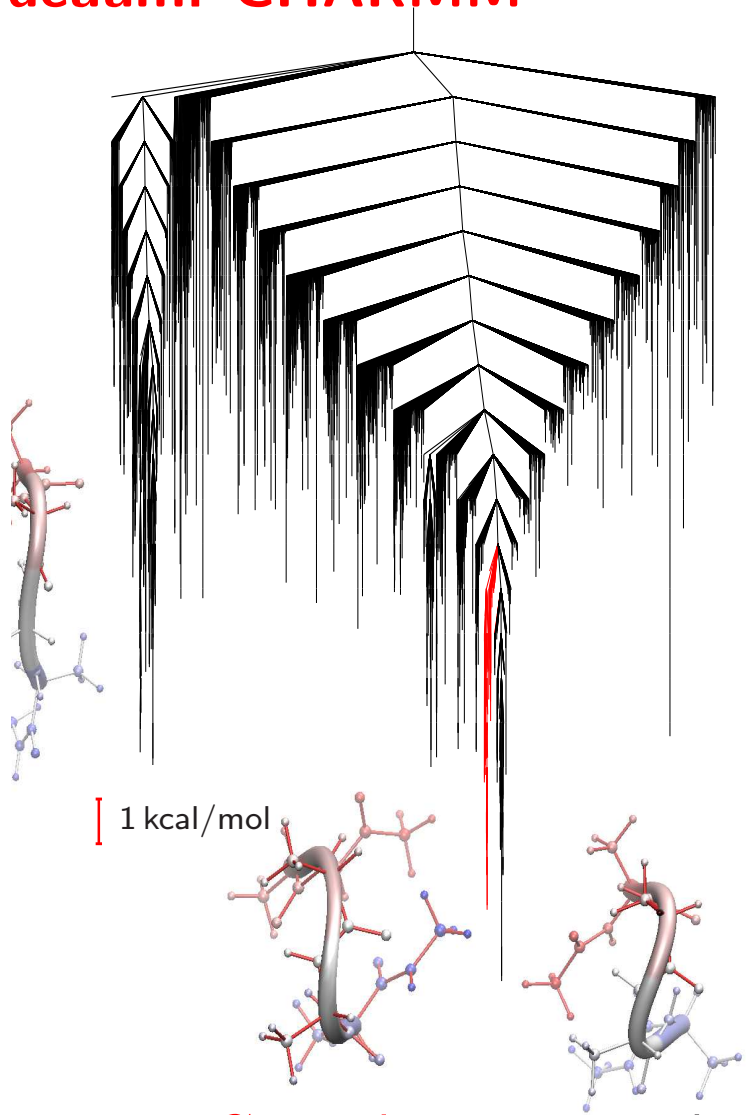

Ala_4 in vacuum (charmm27) has a low temperature C_v peak, corresponding to the hundred or so lowest minima in the disconnectivity graph. The high temperature peak corresponds to the finite system analogue of melting.

Thermodynamics for Ala_4 in Vacuum: AMBER

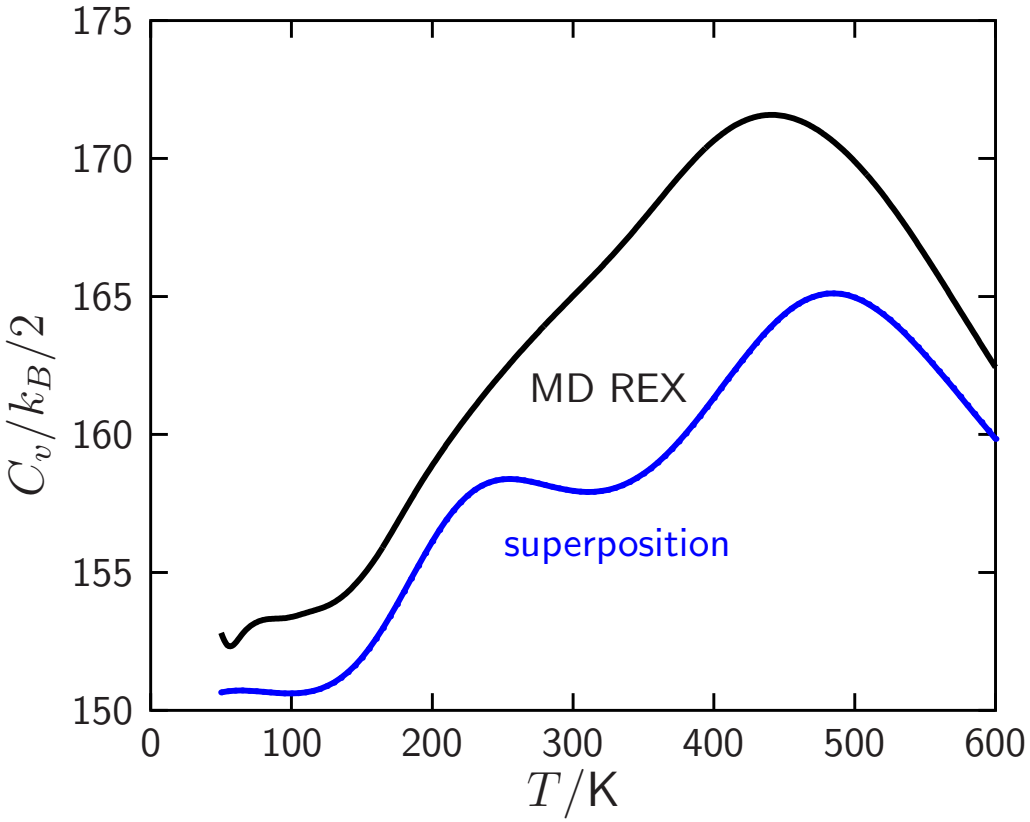

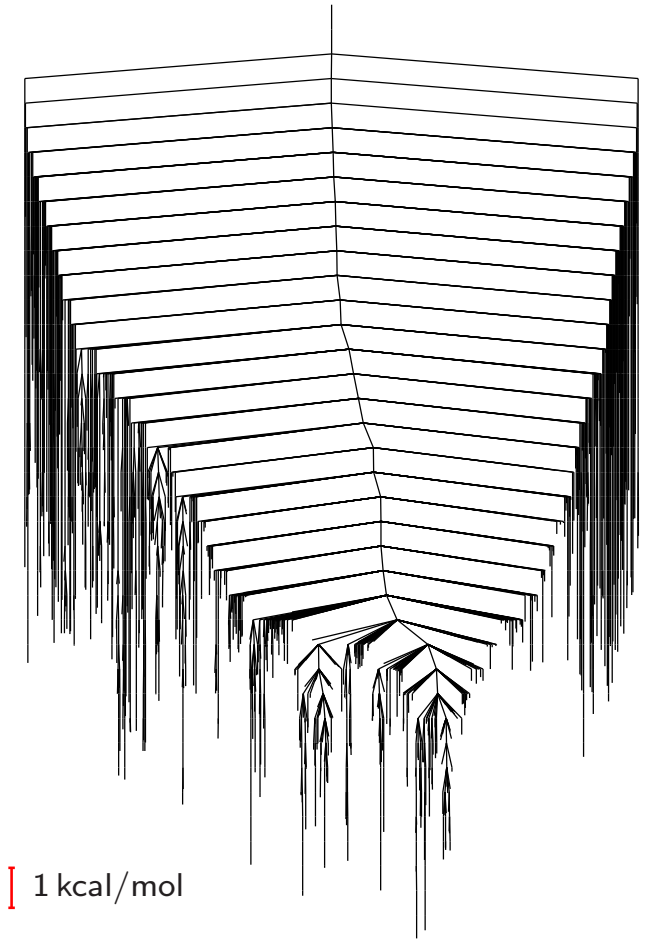

Ala_4 in vacuum (amber99sb) appears to be similar to CHARMM.

Thermodynamics for Ala_4 in Vacuum: AMBER

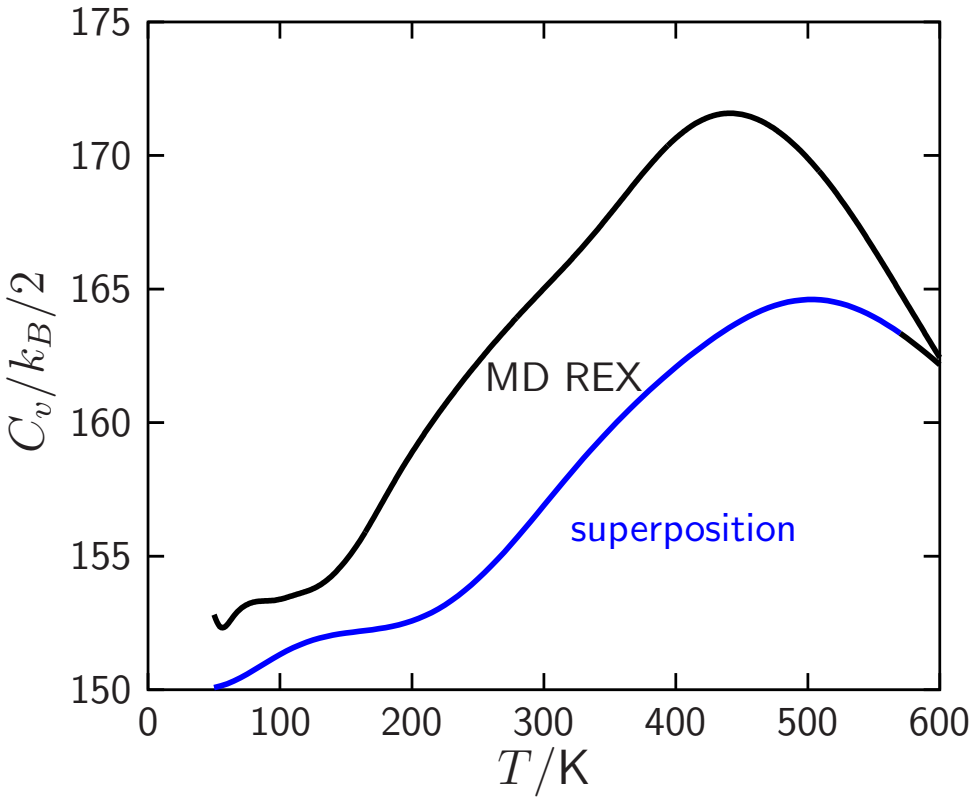

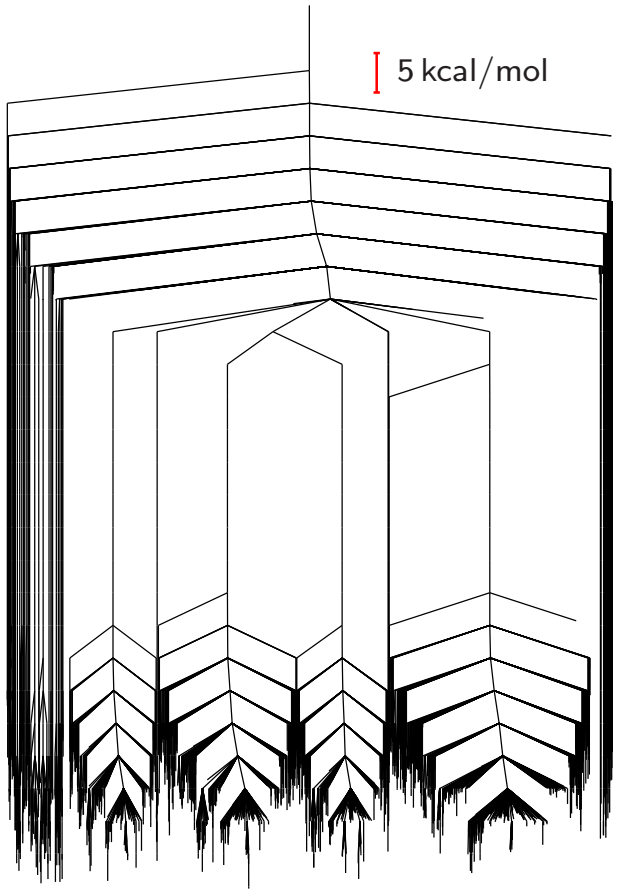

In fact, the global minimum for this potential has a mixture of L and D amino acids. The landscape separates into regions with different L/D composition, spearated by barriers of order 90 kcal/mol.

Exploring Energy Landscapes

Objective: to exploit stationary points (minima and transition states) of the PES as a computational framework (*J. Phys. Chem. B*, **110**, 20765, 2006):

- Basin-hopping for global optimisation (*J. Phys. Chem. A*, **101**, 5111 1997).
  The landscape is transformed via local minimisation: $\widetilde{E}(\mathbf{X}) = \min E(\mathbf{X})$.
  Steps are proposed via geometrical perturbations, and accepted or rejected according to criteria such as the change in energy, e.g. via Metropolis.
- Basin-sampling for global thermodynamics (*J. Chem. Phys.*, **124**, 044102, 2006).
  This approach uses the superposition method, where the total partition function is written as a sum over minima, $Z(T) = \sum_a Z_a(T)$.
- Discrete path sampling for global kinetics (*Mol. Phys.*, **100**, 3285, 2002).
  Transition state searches are used to construct a kinetic transition network. Rate constants are extracted assuming Markovian dynamics and a unimolecular rate theory for individual minimum-to-minimum transitions.

Geometry Optimisation

Minimisation: Nocedal's algorithm, LBFGS, with line searches removed.

Transition states: single-ended searches use hybrid eigenvector-following ('Defect Migration in Crystalline Silicon', *Phys. Rev. B*, **59**, 3969, 1999); double-ended searches use the doubly-nudged elastic band approach (*J. Chem. Phys.*, **120**, 2082, 2004; *cf.* Henkelman and Jónsson).

The `GMIN` (global optimisation), `OPTIM` (transition states and pathways) and `PATHSAMPLE` (discrete path sampling) programs are available under the Gnu General Public License. Access to the svn source can be arranged for developers. Current svn tarball image: http://www-wales.ch.cam.ac.uk.

Interfaces to many electronic structure codes are included. Example: split interstitial migration in crystalline silicon (*Chem. Phys. Lett.*, **341**, 185, 2001).

Discrete Path Sampling (*Mol. Phys.*, **100**, 3285, 2002; **102**, 891, 2004).

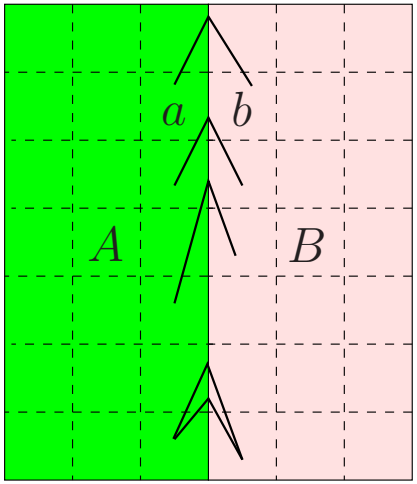

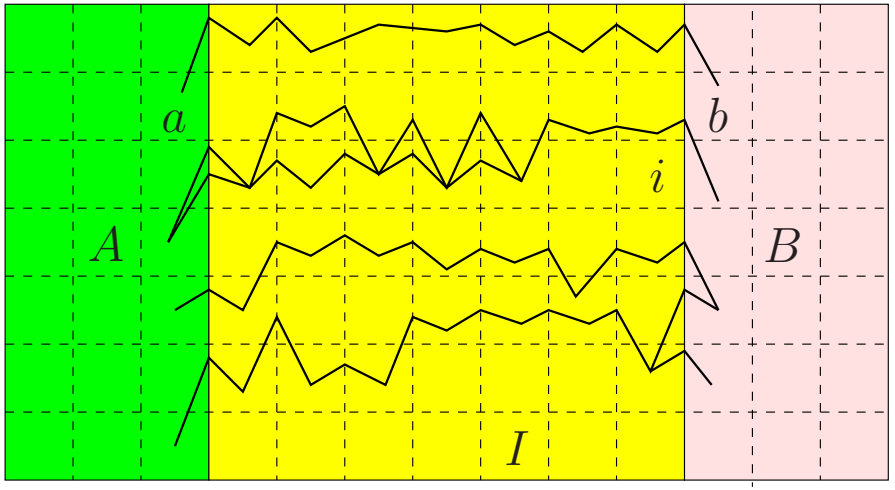

no intervening minima

$$\frac{p_a(t)}{p_{a'}(t)} = \frac{p_a^{\rm eq}}{p_{a'}^{\rm eq}} \qquad \dot{p}_i(t) = 0 \qquad \frac{p_b(t)}{p_{b'}(t)} = \frac{p_b^{\rm eq}}{p_{b'}^{\rm eq}}$$

Phenomenological $A \leftrightarrow B$ rate constants can be formulated as sums over discrete paths, defined as sequences of local minima and the transition states that link them, weighted by equilibrium occupation probabilities, $p_b^{\rm eq}$:

$$k_{AB}^{\rm SS} = \frac{1}{p_B^{\rm eq}} \sum_{a \leftarrow b} P_{ai_1} P_{i_1 i_2} \cdots P_{i_{n-1} i_n} P_{i_n b} \tau_b^{-1} p_b^{\rm eq} = \frac{1}{p_B^{\rm eq}} \sum_{b \in B} \frac{C_b^A p_b^{\rm eq}}{\tau_b},$$

where $P_{\alpha\beta}$ is a branching probability and C_b^A is the committor probability that the system will visit an A minimum before it returns to the B region.

Discrete path sampling builds connected databases of stationary points that are relevant to global kinetics (*Int. Rev. Phys. Chem.*, **25**, 237, 2006).

The paths that make the largest contributions to k_{AB}^{SS} can be extracted using the Dijkstra or recursive enumeration algorithms, using edge weights $-\ln P_{\alpha\beta}$ (*J. Chem. Phys.*, **121**, 1080, 2004; *J. Phys. Chem. B*, **112**, 8760, 2008).

A hierarchy of expressions can be obtained for the rate constants:

$$k_{AB}^{\mathrm{SS}} = \frac{1}{p_B^{\mathrm{eq}}} \sum_{b \in B} \frac{C_b^A p_b^{\mathrm{eq}}}{\tau_b}, \quad k_{AB}^{\mathrm{NSS}} = \frac{1}{p_B^{\mathrm{eq}}} \sum_{b \in B} \frac{C_b^A p_b^{\mathrm{eq}}}{t_b}, \quad k_{AB} = \frac{1}{p_B^{\mathrm{eq}}} \sum_{b \in B} \frac{p_b^{\mathrm{eq}}}{\mathcal{T}_{Ab}}.$$

τ_b, t_b and $\mathcal{T}_{Ab}$ are the mean waiting times for a transition from b to an adjacent minimum, to any member of $A \cup B$, and to the A set, with $\tau_b \leq t_b \leq \mathcal{T}_{Ab}$.

k_{AB} is formally exact within a Markov assumption for transitions between the states, which can be regrouped. Additional approximations come from incomplete sampling, and the densities of states and the unimolecular rate theory used to describe the local thermodynamics and kinetics.

Rates from Graph Transformation (*JCP*, **124**, 234110, 2006; **130**, 204111, 2009)

The deterministic graph transformation procedure is non-stochastic and non-iterative. Minima, x, are progressively removed, while the branching probabilities and waiting times in adjacent minima, β, are renormalised:

$$P'_{\gamma\beta} = P_{\gamma\beta} + P_{\gamma x}P_{x\beta}\sum_{m=0}^{\infty} P_{xx}^{m} = P_{\gamma\beta} + \frac{P_{\gamma x}P_{x\beta}}{1-P_{xx}}, \qquad \tau'_{\beta} = \tau_{\beta} + \frac{P_{x\beta}\tau_{x}}{1-P_{xx}}.$$

Each transformation conserves the MFPT from every reactant state to the set of product states with an execution time independent of temperature:

kT/K	$\Delta F_{\mathrm{barrier}}$	N_{min}	N_{ts}	NGT/s	SOR/s	KMC/s
298	5.0	272	287	8	13	85,138
298	4.5	2,344	2,462	8	217,830	
1007	-	40,000	58,410	35	281	1,020,540
1690	-	40,000	58,410	39	122,242	

Discrete Path Sampling Examples I

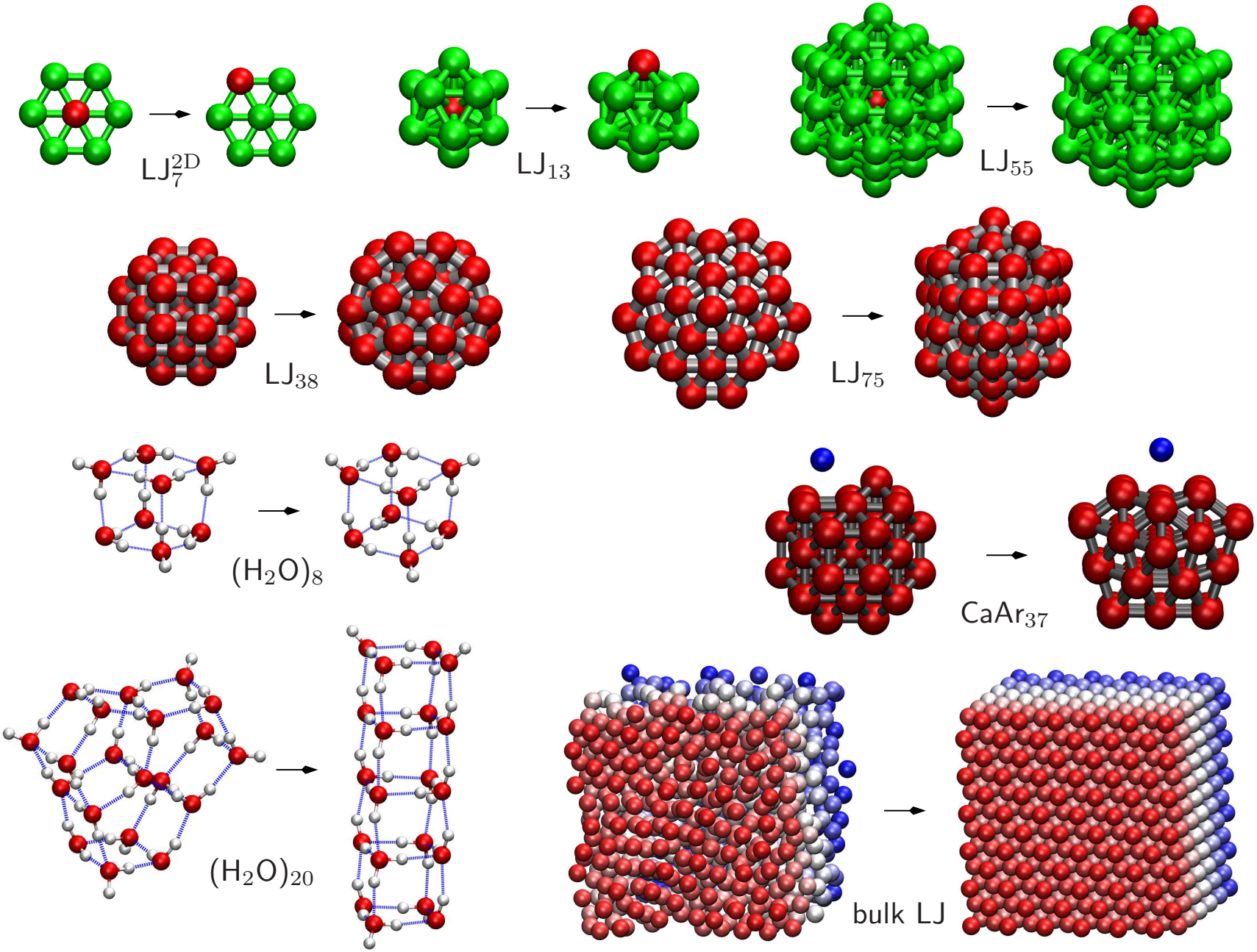

Discrete Path Sampling Examples II

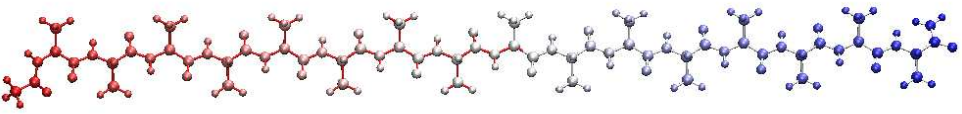

Ala_{16}

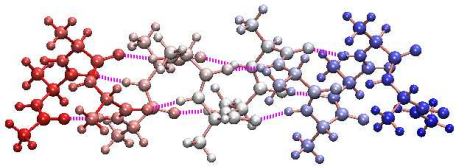

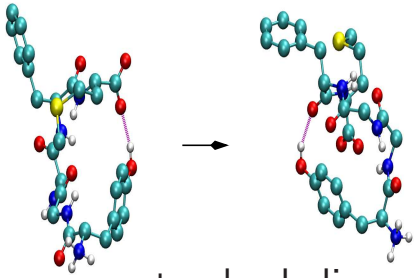

met-enkephalin

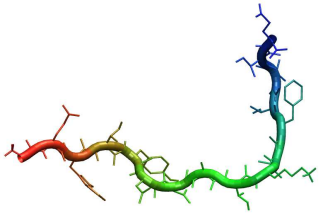

GB1
hairpin

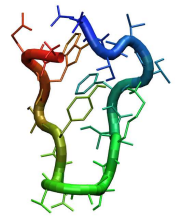

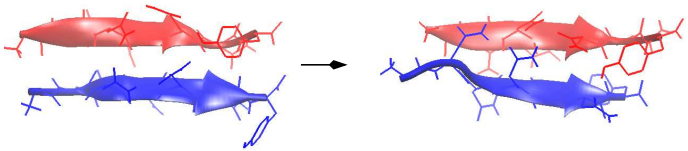

GNNQQNY

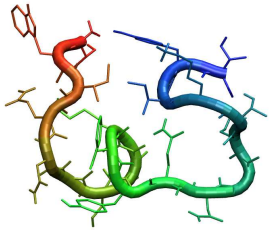

beta3s

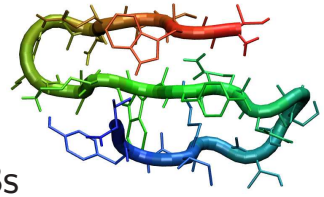

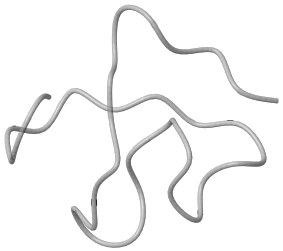

villin

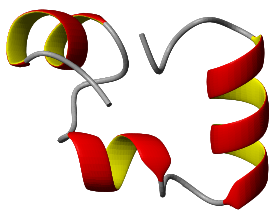

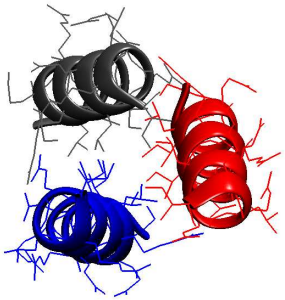

ccbeta

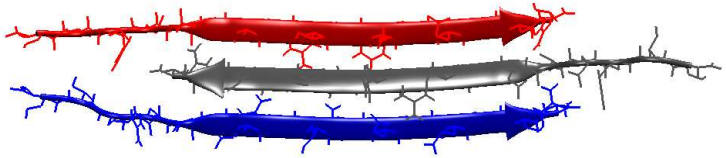

NtrC

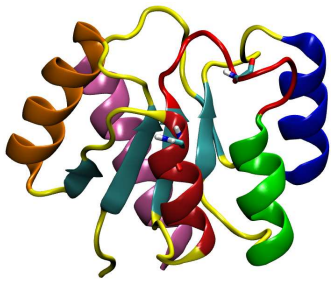

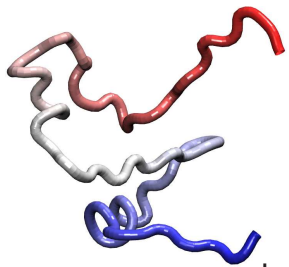

1UAM
trefoil knot

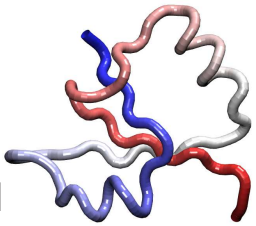

Broken Ergodicity: LJ_{38} (*Phys. Rev. E*, **60**, 3701, 1999)

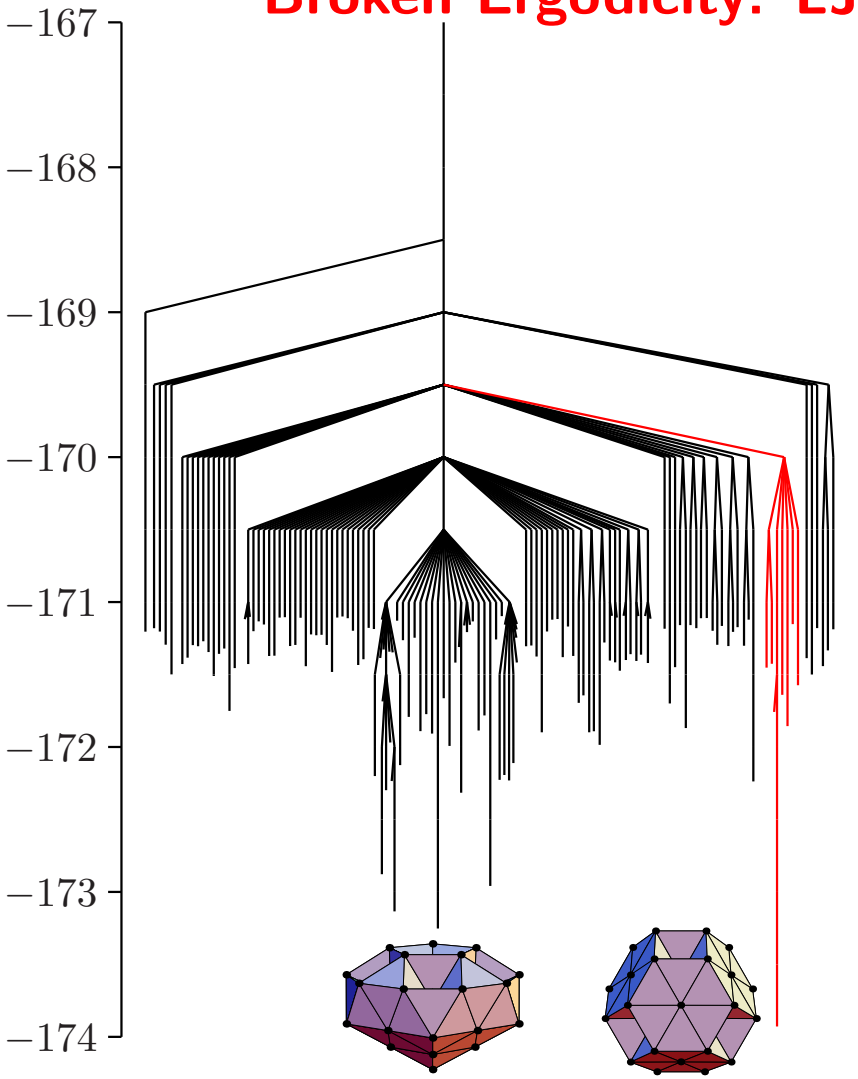

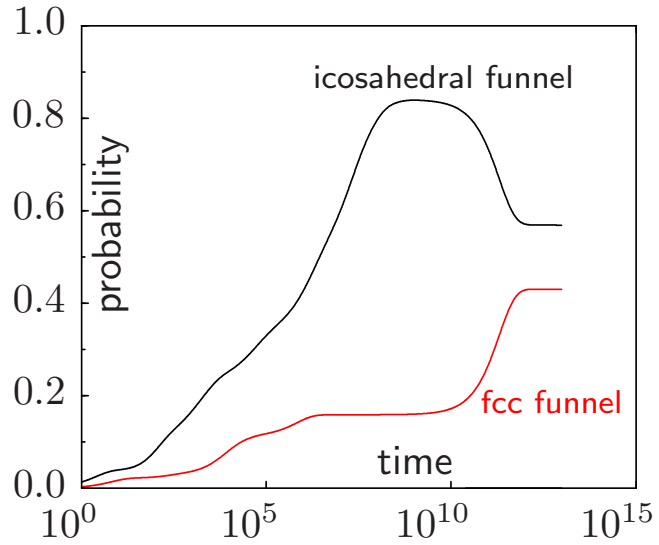

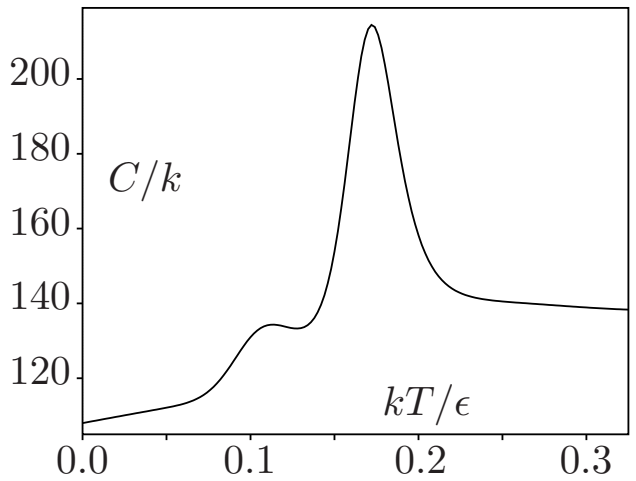

LJ_{38} exhibits a double funnel due to competition between icosahedral and truncated octahedral morphologies. The interconversion rate for Ar_{38} is calculated as $55\,s^{-1}$ at 14 K where a solid-solid transition occurs.

THE JOURNAL OF CHEMICAL PHYSICS **135**, 034108 (2011)

Simulating structural transitions by direct transition current sampling: The example of LJ_{38}

Massimiliano Picciani,[1,a)] Manuel Athènes,[1] Jorge Kurchan,[2] and Julien Tailleur[3]
[1]*CEA, DEN, Service de Recherches de Métallurgie Physique, F-91191 Gif-sur-Yvette, France*
[2]*CNRS; ESPCI, 10 rue Vauquelin, UMR 7636 PMMH, 75005 Paris, France*
[3]*School of Physics of Astronomy, SUPA, University of Edinburgh, The King's Buildings, Mayfield Road, EH9 3JZ Edinburgh, United Kingdom*

(Received 2 March 2011; accepted 21 June 2011; published online 20 July 2011)

Another attempt to study the transitions between the two funnels of LJ_{38} relies on the use of transition path sampling.[33] Because of the number of metastable states separating the two main basins, the traditional shooting and shifting algorithm failed here, despite previous success for smaller LJ clusters.[39] The authors thus developed a two-ended approach which manages to successfully locate reaction paths between the two basins: they started from a straight trial trajectory linking the two minima, and obtained convergence towards trajectories of energies similar to those obtained in the discrete path sampling approach.[33] Although the authors point out the lack of ergodicity in the sampling within their approach and the sensitivity on the "discretization" of the trajectories, this is nevertheless a progress and the main drawback remains the high computational cost (the work needed 10^5 h of central processing unit (cpu) time) to obtain such converged trajectories. In contrast, the simulations we present below required less than 10^2 h of cpu time.

Glassy Landscapes (*J. Chem. Phys.*, **129**, 164507, 2008)

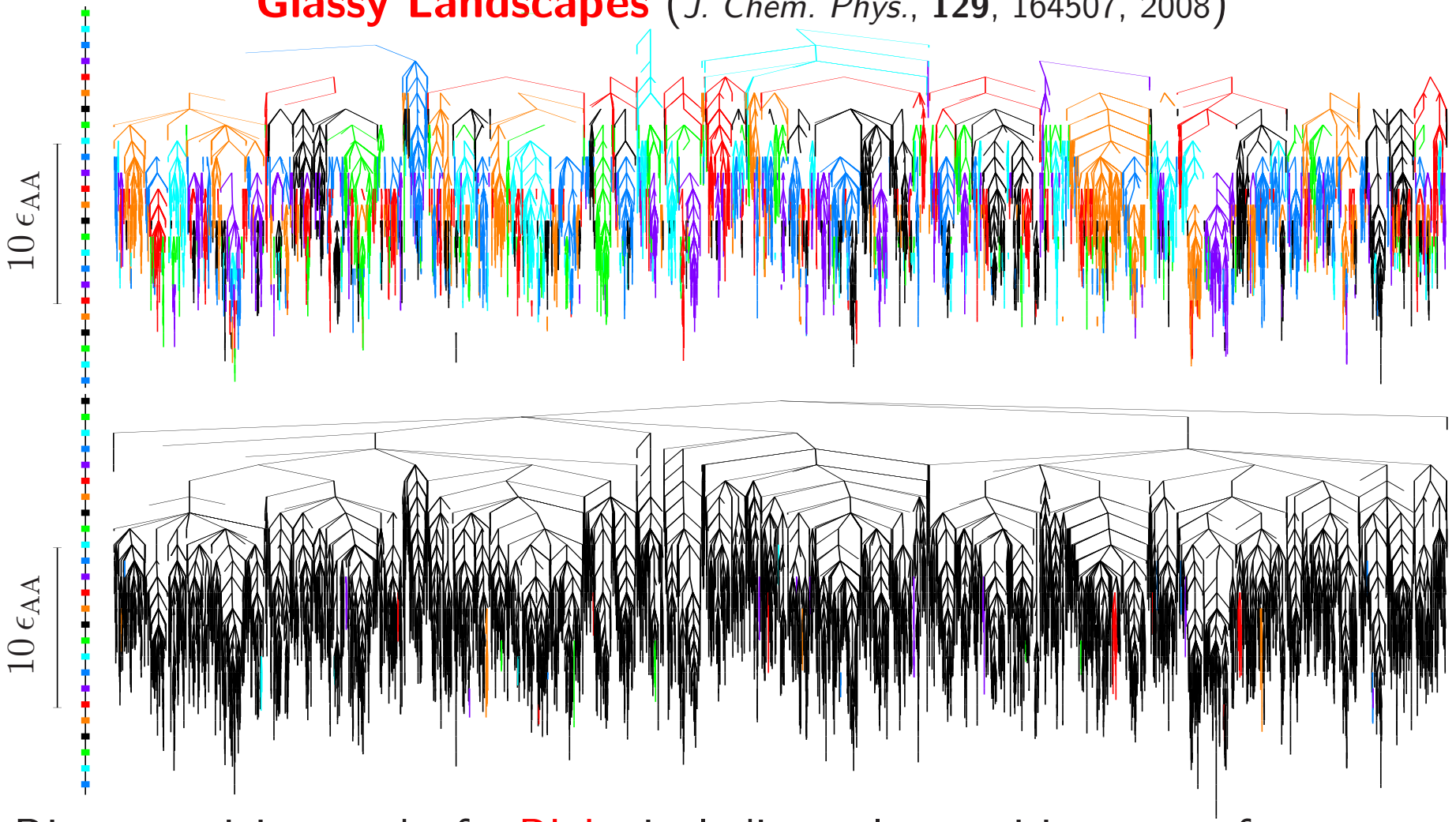

Disconnectivity graphs for BLJ_{60} including only transition states for noncage-breaking (top) and cage-breaking (bottom) paths. Changes in colour indicate disjoint sets of minima. Cage-breaking transitions, defined by two nearest-neighbour changes, define a higher order metabasin structure.

Nanodevices (*Soft Matter*, **7**, 2325, 2011)

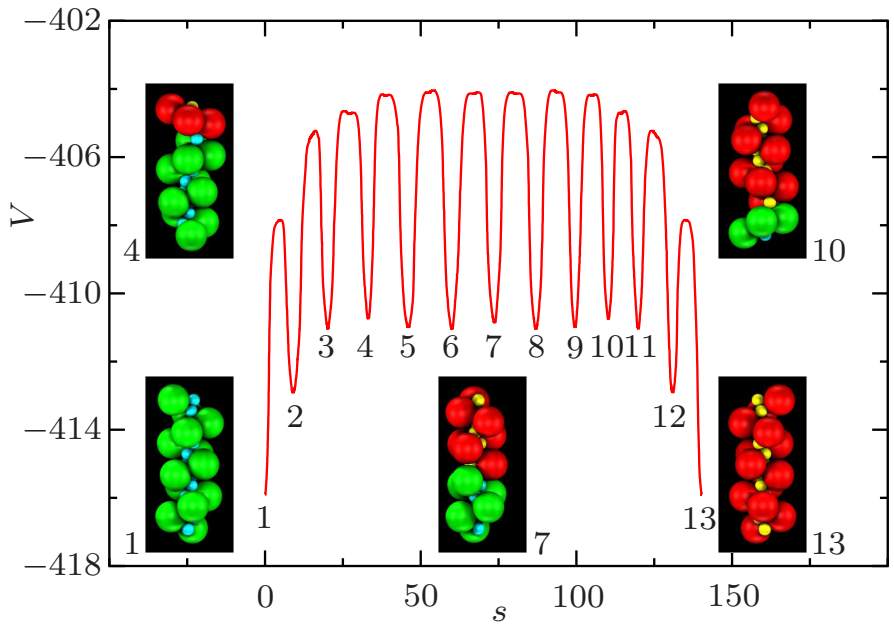

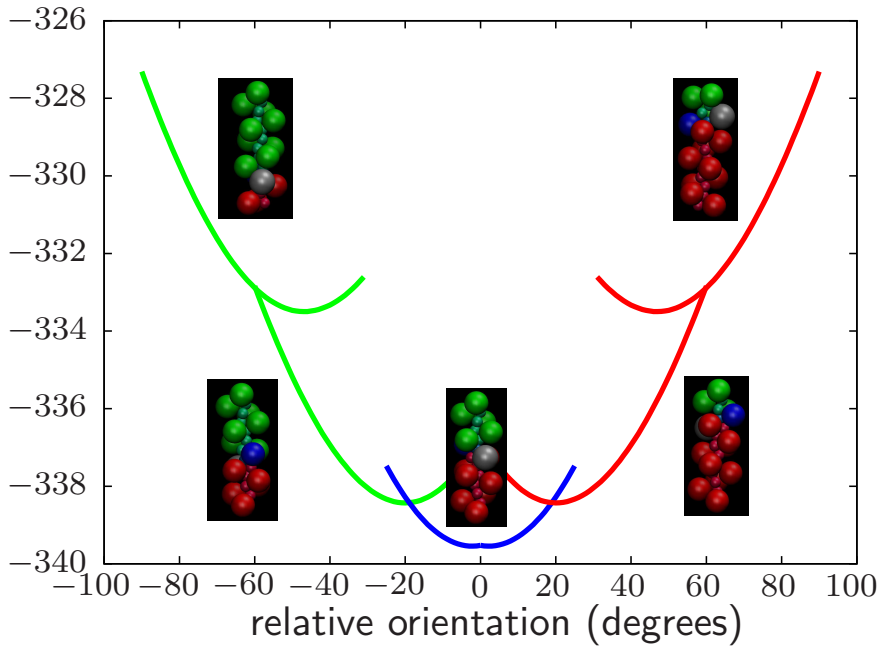

Coupled linear and rotary motion has been characterised for a helix composed of 13 asymmetric dipolar dumbbells in the presence of an electric field.

The helix changes handedness as the boundary between segments propagates along the strand via successive steps that switch the dumbbells.

Applying a torque to the helix systematically drives a defect and associated ligand along the chain; moving the ligand could produce rotatory motion.

Folding and Pulling for Protein L and Protein G

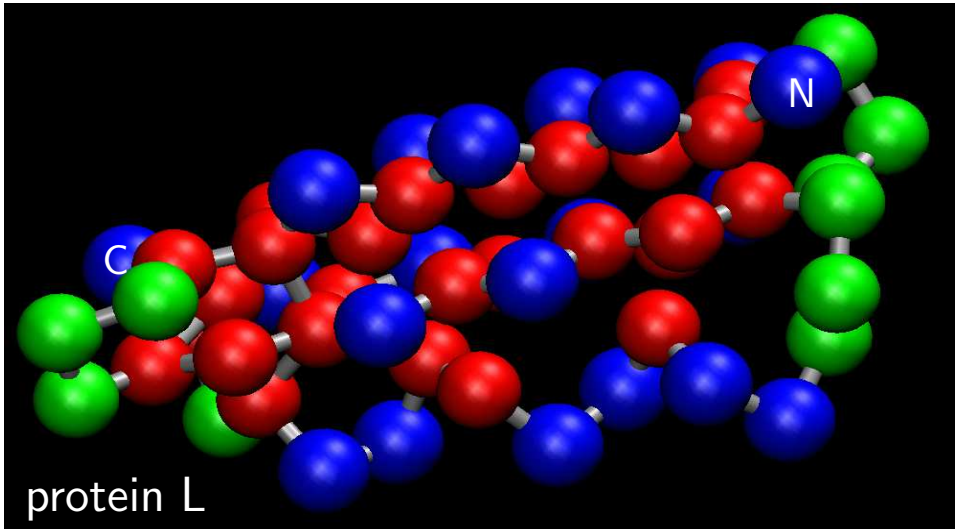

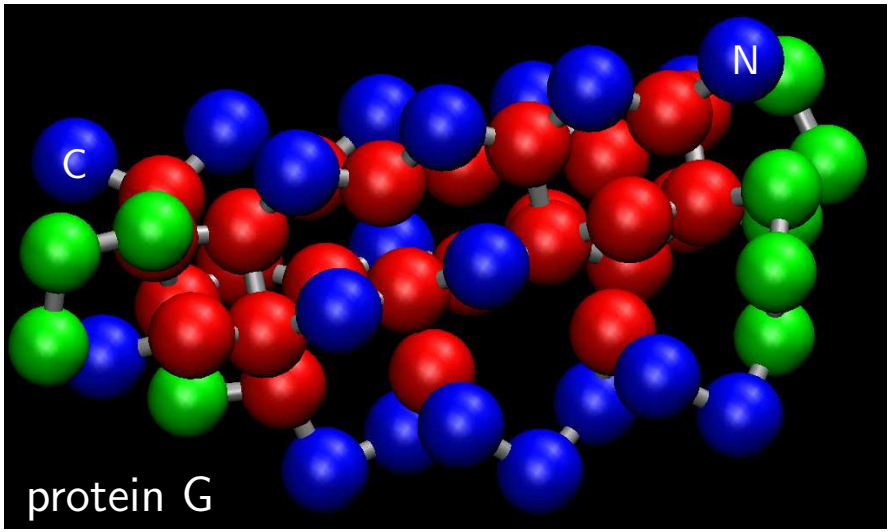

Folding pathways and the evolution of the energy landscape as a function of static force have been analysed for protein L and protein G using the sequence-dependent BLN model of Brown, Fawsi and Head-Gordon.

Single site residues: B=hydrophobic, L=hydrophilic, and N=neutral.

Both proteins have a central α-helix packed against a four-stranded β-sheet composed of two β-hairpins, despite little sequence identity. Protein L forms the N-terminal hairpin 1 first, followed by the C-terminal hairpin 2, but the order is reversed for protein G, which exhibits an early intermediate.

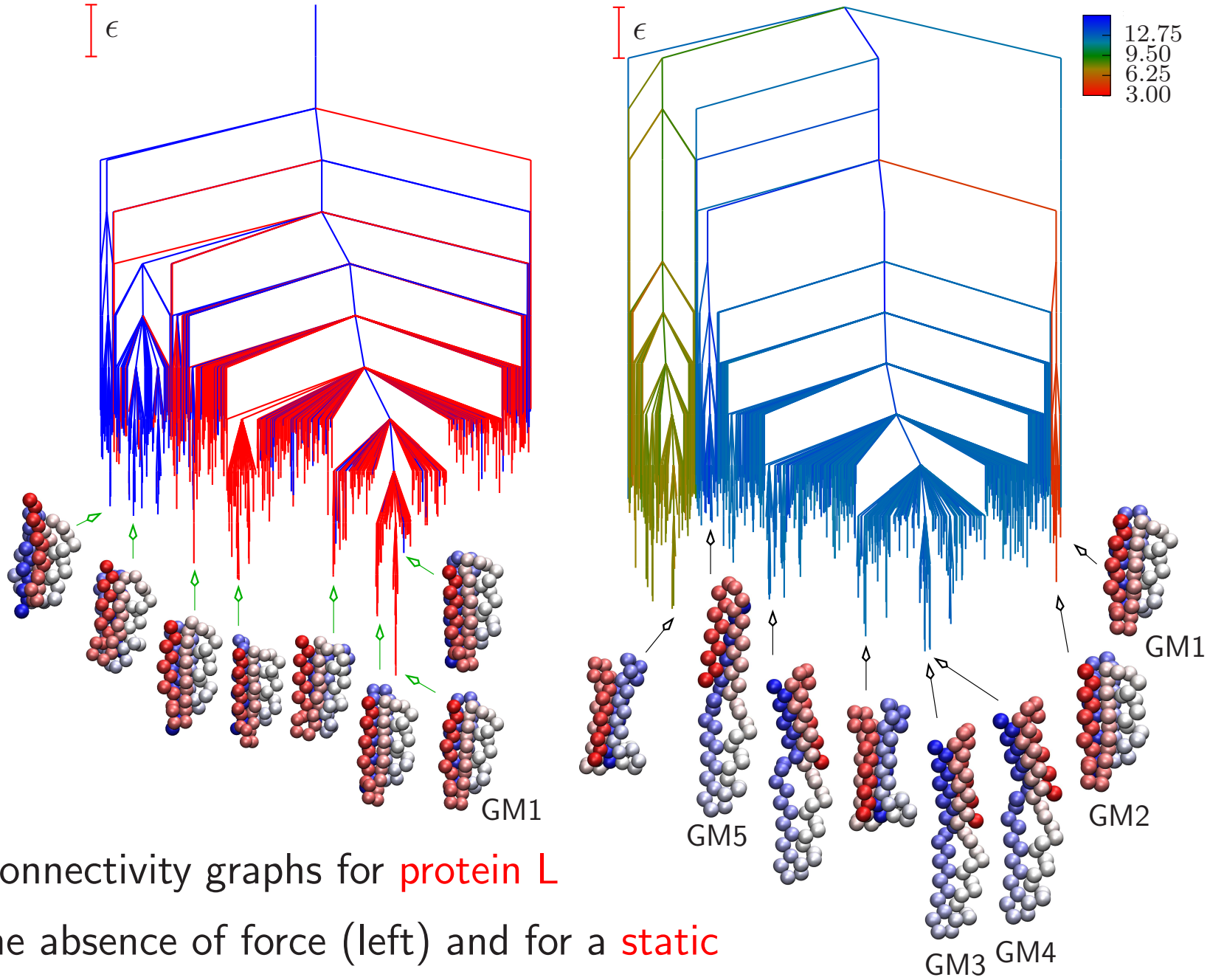

Disconnectivity graphs for protein L in the absence of force (left) and for a static pulling force (right) applied between beads 10 and 32.

Regrouping Stationary Point Databases

Lumping local minima together (recursively) if they are separated by low barriers or fast rates reduces the dimension of the kinetic transition network (*J. Chem. Phys.*, **123**, 234901, 2005; *J. Chem. Phys.*, **121**, 1080, 2004). It also provides a self-consistent definition of products and reactants.

The occupation probability and free energy of a group of minima, J are

$$p_J^{\mathrm{eq}}(T) = \sum_{j \in J} p_j^{\mathrm{eq}}(T) \quad \text{and} \quad F_J(T) = -kT \ln \sum_{j \in J} Z_j(T),$$

and the free energy of the transition states connecting J and L is then

$$F_{LJ}^{\dagger}(T) = -kT \ln \sum_{(lj)^{\dagger}} Z_{lj}^{\dagger}(T), \qquad l \in L,\ j \in J,$$

$$\text{with} \quad k_{LJ}^{\dagger}(T) = \sum_{(lj)^{\dagger}} \frac{p_j^{\mathrm{eq}}(T)}{p_J^{\mathrm{eq}}(T)} k_{lj}^{\dagger}(T) = \frac{kT}{h} \exp\left[-\frac{\left(F_{LJ}^{\dagger}(T) - F_J(T) \right)}{kT} \right].$$